Available online at www.sciencedirect.com

ScienceDirect

Energy Procedia 126 (201709) 517–524

Energy Procedia

www.elsevier.com/locate/procedia

72nd Conference of the Italian Thermal Machines Engineering Association, ATI2017, 6-8 September 2017, Lecce, Italy

Numerical simulation of a finned-tube LHTES system: influence of the mushy zone constant on the phase change behaviour

Simone Arena[a*], Efisio Casti[a], Jaume Gasia[b], Luisa F. Cabeza[b], Giorgio Cau[a]

[a]*Università degli studi di Cagliari, Dipartimento di Ingegneria Meccanica, Chimica e dei Materiali, via Marengo 2, 09123, Cagliari, Italy*
[b]*GREA Innovació Concurrent, INSPIRES Research Centre, Universitat de Lleida, Pere de Cabrera s/n, 25001 Lleida, Spain*

Abstract

This work presents a numerical investigation on latent heat thermal energy storage (LHTES) systems during the phase change process. The numerical analysis, based on the apparent heat capacity formulation, was carried out through a two-dimensional axisymmetric numerical model developed by means of the COMSOL Multiphysics software. A thermal energy storage system based on the configuration of a double tube heat exchanger with finned surfaces was used as an experimental test case and the commercial paraffin RT35 was selected as phase change material (PCM). The influence of the heat transfer by convection, in particular the influence of the term describing the mushy zone in the momentum equation, was investigated during the whole charge and discharge processes. Three different values of the constant A_{mush}, equals to 10^4, 10^6 and 10^8 were selected as well as two different values of the HTF volumetric flow rate were adopted in order to reproduce both laminar and turbulent flow regimes. The results are reported in terms of temperature, melting fraction and phases evolution during the whole melting and solidification processes, and compared to previous experimental tests carried out in the laboratories of the University of Lleida, Spain. A good agreement with the experimental results was obtained showing that the mushy zone constant has a significant influence on the interface shape and motion. The results show that large values of A_{mush} determine an increase of the mushy region reducing the natural convection effects during the charge phase. Thus, the proper evaluation of the mushy zone constant allows providing a deeper understanding of the phase change behaviour, resulting in an important parameter for accurate modelling of LHTES systems.

Peer-review under responsibility of the scientific committee of the 72nd Conference of the Italian Thermal Machines Engineering Association

Keywords: PCM, Thermal Energy Storage; Mushy zone constant; Latent Heat; Numerical simulation.

* Corresponding author. Tel.: +39-0706755741; fax: +39-0706755717.
E-mail address: simonearena@unica.it

1876-6102
Peer-review under responsibility of the scientific committee of the 72nd Conference of the Italian Thermal Machines Engineering Association
10.1016/j.egypro.2017.08.237

1. Introduction

Thermal energy storage (TES) systems are an effective solution to improve energy efficiency and to compensate fluctuations and intermittence that affects renewable energy and other non-programmable energy sources. For low temperature applications, the most common TES systems are of sensible heat type and water is the most widely used material due to its availability, low cost, safety and transport ability. Nowadays, latent heat thermal energy storage systems (LHTES) using phase change materials (PCM) is an attractive option in such applications due to their higher energy storage density compared to the sensible heat storage and the nearly isothermal behaviour during the phase change process which allow lower temperature swing [1].The development of a LHTES system involves the understanding of the phase change phenomena, the evaluation of heat transfer mechanisms in the PCM during solid-to-liquid phase transition and the design of the devices used for containing the PCM. Concerning the analysis of heat transfer problems in phase change process, several methodologies have been developed and used for modelling LHTES since the heat transfer mechanisms can influence the accuracy of the thermal performance prediction. From literature on LHTES systems, several researches [2–6] investigate the role of natural convection that occurs in the phase transition of a PCM during thermal energy storage evaluating the influence and the effects on the phase change process. In fact, when the PCM inside the TES system is changing phase from solid to liquid, natural convection is produced due to density difference within the fluid and buoyancy forces. This difference would result from temperature and/or concentration gradients in the liquid phase. Liquid motion in the PCM melted region is a much more complicated problem that requires the simultaneous solution of the continuity, momentum and energy equations. The correct evaluation of the phenomena within the mushy zone has been the subject of numerous discussions in recent literature. Shokouhmand et al. [7] carried out an experimental investigation on melting heat transfer characteristics of lauric acid, Shmueli and Ziskind [8] studied the melting process of a PCM in a vertical circular tube focusing on the mushy zone, Groulx et al. [9] analyzed the effect of the mushy zone constant on the overall simulation results of a melting PCM body using a simple rectangular geometry. More recently, Kumar and Krishna [10] studied the influence of the mushy zone constant on the melting characteristics of gallium in a rectangular cavity.

In this work, a two dimensional axysimmetric numerical model of a small-scale LHTES system based on double tube heat exchanger configuration with fins was implemented in the COMSOL Multiphysics platform considering the influence of the mushy zone constant A_{mush} on different characteristic parameters such as temperature, melting fraction, and shape and motion of the phase transition front. The mushy zone is the region where the liquid fraction lies between 0 and 1, i.e. in which a mixture of both solid and molten material co-exist. This region is treated as a porous medium in which the porosity decreases from 1 (liquid PCM) to 0 (solid PCM), resulting in the drop of velocities to zero, and it is modelled by the Carman-Kozeny equation. However, its exact evaluation is still the subject of discussion since recent literature asserts that this parameter has values ranging from 10^3 to nearly 10^{10} [9] depending on morphology or material used. This analysis presents a comparison between experimental and simulation results obtained by adopting three different values of the constant A_{mush}, equals to 10^4, 10^6 and 10^8. Two different experimental tests were reported considering two HTF volumetric flow rate values in order to reproduce both laminar and turbulent flow regimes.

Nomenclature

A_{mush}	Mushy zone constant [kg/s]
C_p	Specific heat capacity [J/kg·K]
F	Force [N]
g	Gravity [m/s^2]
k	Thermal conductivity [W/m·K]
L_f	Latent heat of fusion [J/kg]
P	Pressure [Pa]
t	Time [s]
T	Temperature [K]
T_m	PCM phase change temperature [K]
u	Velocity [m/s]

Greek symbols

α	Mass fraction
β	Thermal expansion coefficient [1/K]
ΔT_m	Phase change temperature range [K]
ϵ	Numerical constant
θ	Fraction of phase before transition
μ	Dynamic viscosity [Pa·s]
ρ	Density [kg/m^3]

Abbreviations

HTF	Heat Transfer Fluid
LHTES	Latent Heat Thermal Energy Storage
PCM	Phase Change Material

2. Material and method

2.1. Experimental set-up and phase change material selection

Experimental tests were carried out in the laboratories of the University of Lleida (Spain), on a small scale heat exchanger used as a TES system [12]. Fig. 1(a) shows a schematic of the experimental set-up. The set-up consists of a thermostatic bath HUBER K25 that controls the water (HTF) inlet temperature, a water pump WILO and a series of valves to control water flow rate, a digital flow meter Badger Metter Prime Advanced (range of 0.85–17 l/min, accuracy of 0.25% for velocities below 5 m/s and 1.25% for higher values), and a system for temperature measurements based on Pt100 DIN-B probes. Both temperature and flow rate readings are collected in a computer via data acquisition system STEP DL01-CPU. Working conditions were chosen to achieve temperature gradients of 25 °C and 15 °C between HTF inlet and PCM transition temperature during charge and discharge respectively.

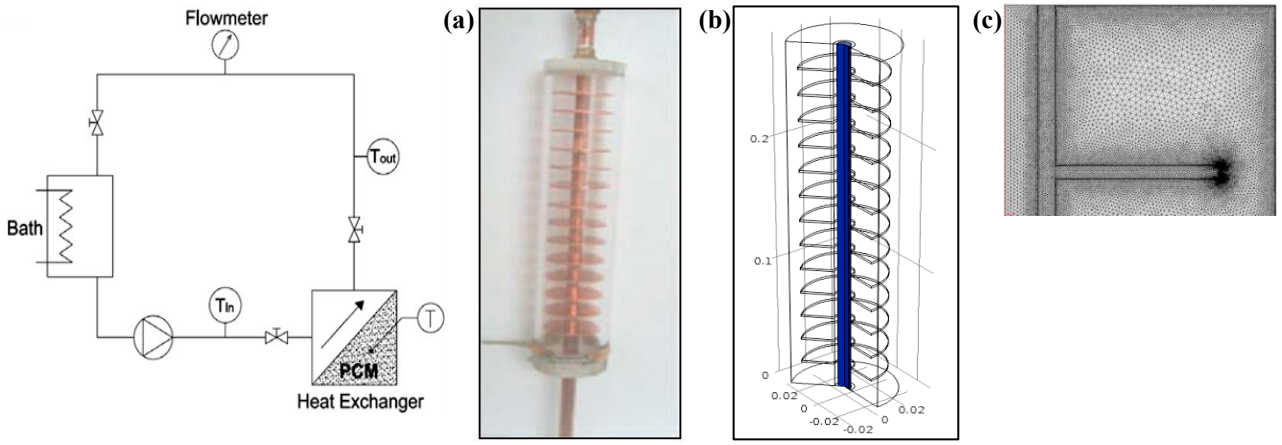

Fig. 1. (a) Scheme of experimental set-up, (b) double tube heat exchanger with fins, (c) geometric configuration of the TES system implemented in COMSOL Multiphysics, (d) adopted mesh.

Table 1. Summary of charge and discharge experiments carried out.

	Experiment 1		*Experiment 2*	
	Charge	Discharge	Charge	Discharge
Volumetric flow rate (m^3/h)	0.03	0.4	0.4	0.4
Reynolds Number	1600	22000	22000	22000
HTF temperature (°C)	60	20	60	20

Table 2. Geometrical characteristics of the storage system and properties of Rubitherm RT35 [2,12]

	Units	*Value*
External diameter of HTF tube	mm	12
Height	mm	280
Thickness of HTF tube	mm	2
External diameter of PCM tube	mm	65
Thickness of PCM tube	mm	6
Number of fins	-	13
Diameter fins / Thickness fins	mm	52 / 1.5
Heat transfer area	m^2	0.065
PCM mass	kg	0.5
	Solid	*Liquid*
Density (kg/m^3)	880	760
Specific heat capacity (J/kg·K)	1800	2400
Thermal conductivity (W/m·K)	0.2	0.2
Phase change temperature	35 °C	
Range of transition temperature	3 °C	
Latent heat	157 kJ/kg	

Commercial paraffin RT35 from Rubitherm® Technologies GmbH was selected and used as PCM filling the annulus of the heat exchanger, and water circulated through the inner tube as heat transfer fluid. Two experiments were carried out considering two values of the HTF volumetric flow rate in order to reproduce both laminar and turbulent flow regimes. In particular, the discharge phase was characterized by turbulent regime for both experiments, while

the charge phase was characterized by laminar and turbulent regimes for Experiment 1 and 2, respectively. In all cases, the HTF enters from the upper side of the TES system. The specific conditions used in the experiments are presented in Table 1. To improve the significance of the experimental result obtained, three different repetitions of the test, using the same initial conditions, were carried out. Subsequently, the analysis on the averaging effect of replication was performed in order to obtain a more accurate estimate of the mean effect and to improve the reliability of the results. Finally, the whole data set of the test closest to the average value was selected as the replication which reflect its experimental worth. The TES system is based on the configuration of double pipe heat exchanger with 13 radial copper fins. Fig. 1(b) shows a picture of the TES system and Fig. 1(c) of the geometric configuration implemented in COMSOL Multiphysics. The inner tube is copper while the outer is made of transparent material (methacrylate) that allows a direct view of the phase transition process. The geometrical characteristics of the TES system and the main physical properties of RT35 [13,14] are reported in Table 2. The potential applications in the operative temperature range (35-40 °C) of this type of TES systems are related to small-size systems, such as, telecommunication devices and home appliances.

2.2. Mathematical model of the PCM-TES

A 2D axisymmetric numerical model was implemented in COMSOL Multiphysics to simulate the transient behaviour of the entire PCM-TES system during the phase change processes [9,15–17] using the equations reported in Table 3. The mathematical model is based on the following assumptions: the HTF velocity profile is fully developed and does not change within a section; uniform temperature at inlet boundary; empirical functions are adopted for describing viscous losses and PCM is bounded by adiabatic external wall. The transition process was modeled using the energy equation, Eq. (1), in accordance with the apparent heat capacity formulation expressed by Eq. (3). The latent heat L_f was introduced as an additional term in the Eq. (3) assuming that the phase change takes place between $(T_m - \Delta T_m/2)$ and $(T_m + \Delta T_m/2)$. In this temperature range the material phase is modelled by a smoothed function θ, representing the fraction of phase before transition. The value of this function is equal to 1 for temperatures lower than $(T_m - \Delta T_m/2)$ and to 0 for temperatures higher than $(T_m + \Delta T_m/2)$. For this work, the temperature range of phase transition ΔT_m was considered constant and equal to 3 °C. The mass fraction α (Eq. 3) is equal to $-1/2$ before transition and $1/2$ after transition and it is defined by Eq. (4). The equivalent heat conductivity and density of the PCM were obtained by Eqs. (5) and (6).

Table 3. Equations used in the model to simulate the entire PCM-TES system during the phase change processes.

$$\boldsymbol{\rho C_p \frac{\partial T}{\partial t} + \rho C_p u \cdot \nabla T = \nabla \cdot (k \nabla T)} \quad (1)$$

$$\boldsymbol{\frac{\partial \rho u}{\partial t} + \rho(u \cdot \nabla)u - \nabla \cdot [\mu(\nabla u + (\nabla u)^{T})] + \nabla P = F_b + F_v} \quad (2)$$

$$\boldsymbol{C_p = \frac{1}{\rho}\left[\theta \rho_{phase1} C_{p,phase1} + (1-\theta)\rho_{phase2} C_{p,phase2}\right] + L_f \frac{\partial \alpha}{\partial T}} \quad (3)$$

$$\boldsymbol{\alpha = \frac{1}{2}\frac{(1-\theta)\rho_{phase2} - \theta \rho_{phase1}}{\rho}} \quad (4)$$

$$\boldsymbol{k = \theta k_{phase1} + (1-\theta) k_{phase2}} \quad (5)$$

$$\rho = \theta \rho_{phase1} + (1-\theta)\rho_{phase2} \quad (6)$$

$$F_b = g \rho_l \beta (T - T_m) \quad (7)$$

$$F_v = -A(T) \cdot u \quad (8)$$

$$A(T) = A_{mush} \frac{(1-\theta)^2}{(\theta^3 + \epsilon)} \quad (9)$$

$$\mu(T) = \mu_l \left(1 + A(T)\right) \quad (10)$$

In order to predict the behaviour of the PCM in liquid phase, the continuity and momentum equations, Eq. (1) and Eq. (2), were used. Two different volume forces $\boldsymbol{F_b}$ and $\boldsymbol{F_v}$were introduced in Eq. (2). The first one takes into account the buoyancy force giving rise to natural convection (Boussinesq approximation) according to Eq. (7). The second volume force F_v (Eq. 8) was introduced as a source term in the momentum conservation equation using the Carman-Kozeny equation (Eq. 9) in order to force the Navier-Stokes equation to calculate the velocity in both the liquid and solid PCM domain since the entire PCM was treated as a liquid, even when its temperature was lower than the melting one. Thus, the term F_v induces a gradual increase in velocity from zero in the solid PCM, when the function $A(T)$ assumes very large values, to a finite value in the liquid PCM calculated by Eq. (2), when the

function $A(T)$ approaches to zero. In Eq. (9) the constant ϵ is assumed equal to 10^{-3} to avoid a division by zero when $\theta = 0$ in the solid region. The value of A_{mush} is assumed equal to 10^4, 10^6 and 10^8 in order to understand the effect of this parameter on the simulated transition process of the selected PCM. Furthermore, a modified viscosity (Eq. 10) was used. In Eq. (10), $\mu(T)$ assumes the value of the viscosity of the liquid PCM when $T > (T_m + \Delta T_m/2)$ while it assumes an extremely large value, depending on the A_{mush} value, when $T < (T_m - \Delta T_m/2)$, forcing the PCM (considered constant in liquid state) to behave as a solid [17]. A very fine mesh composed of a free triangular mesh geometry was selected using 255687 elements and 7824 boundary elements (Fig. 1d) with average element quality of 0.9179, in order to achieve a mesh-independent result.

3. Results and discussion

The results obtained for the Experiment 1 during charge and discharge process were analyzed by varying the constant A_{mush} according to the three mentioned values. Concerning Experiment 2, only the A_{mush} value of 10^6 was considered during the charge process, while a complete analysis was carried out during the discharge phase since the same HTF volumetric flow rate was adopted in both experiments. Fig. 2 reports the PCM temperature profiles for the charge (a) and discharge (b) processes. The duration of the charge process for the two experiments was imposed equal to 1600 and 900 seconds, respectively, while the discharge process starts from an initial condition in which the PCM is completely in liquid phase and ends at imposed time equal to 2100 seconds for both the experiments, to validate the current available data [11]. The discharge phase starts considering as initial condition the complete PCM melting within the TES. The temperature measurement was taken in a centered position in the PCM domain, between the fin and the outer wall in the radial direction and half way between inlet and outlet in the axial direction. At first, it can be noticed that the model has a good agreement with the experimental results. Fig. 2(a) shows that the temperature profiles present the same trend by varying the A_{mush} value. At the selected measuring point, the reported curves, especially during charge, suddenly undergo the phase transition when the temperature reaches the value of $T_m - \Delta T_m/2$. This trend also depends on the temperature difference between PCM during transition and HTF at the inlet device, approximately 25 °C during charge and 15 °C during discharge.

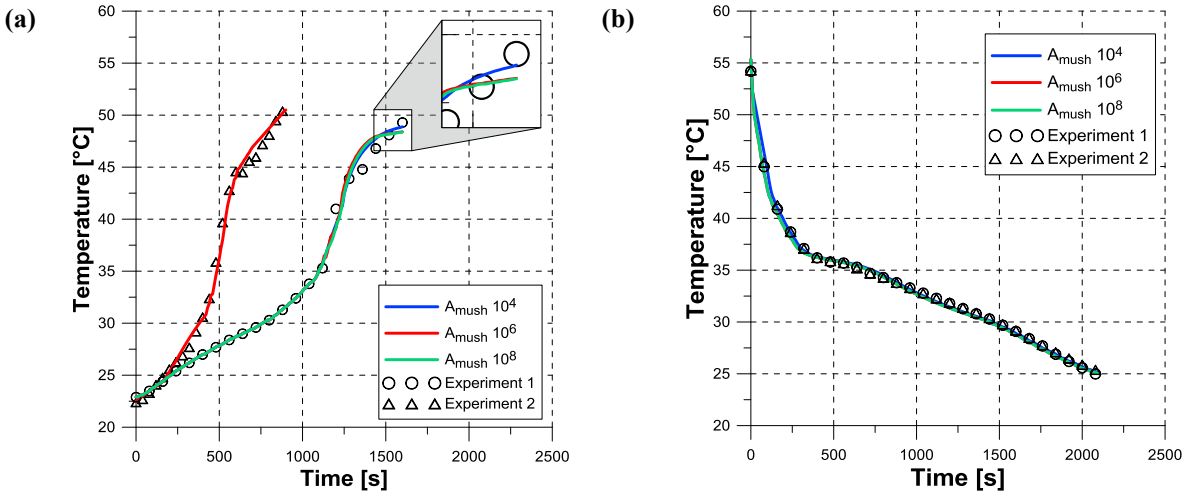

Fig. 2. PCM temperature profile for charge (a) and discharge (b) processes.

In the magnifier, a small difference was detected at the end of the charge phase for the case of $A_{mush} = 10^4$, which presents a slightly higher temperature (about 1°C) with respect to the other two cases considered. Physically, larger values of A_{mush} increase the mushy-zone area reducing the effect of the natural convection and effectively decreasing the overall heat transfer rate through this region. Therefore, a larger temperature difference should be observed between the three cases considered as a result of such a large variation of the mushy zone constant A_{mush} from 10^4 to 10^8. This could be explained since the presence of finned surfaces enhances the internal heat transfer of the system, improving the heat transfer by conduction and further reducing the contribution of convection. Conversely, during discharge (Fig. 2b) the numerical prediction of the three cases with different A_{mush} appear very

close to the experimental results. This can be explained by the different nature of the heat transfer phenomena that take place during melting and solidification. In fact, in case of solidification, conduction is the only heat transfer mechanism, while in case of melting, natural convection occurs in the melt layer dominating the heat transfer process and this generally increases the heat transfer rate compared to the solidification process. Thus, the variation of A_{mush} has a very poor influence in solidification process. Fig. 3 shows the PCM melted fraction versus time for the charge (a) and discharge (b) processes. This parameter is defined as the ratio between the volume of PCM in liquid phase and the total volume occupied by the PCM. By definition, the melting fraction is 0 at the beginning of the charge process and 1 at the beginning of the discharge process.

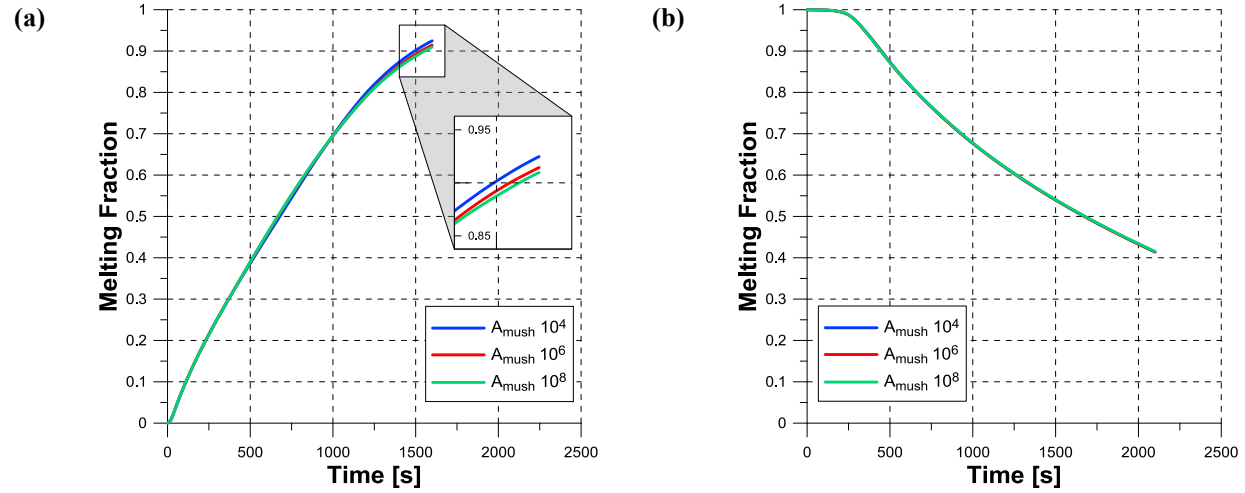

Fig. 3. Melting fraction for charge (a) and discharge (b) processes

As said before, the analysis of the effects of the variation of A_{mush} was carried out only for Experiment 1, thus the melting fraction curves obtained during charge (Fig. 3a) refer only to this experiment. During discharge, the melting fraction curves (Fig. 3b) are valid for both experiments since the same HTF volumetric flow rate was assumed. At the end of the established charging time (1600 s), the value of the melting fraction is approximately 0.91 for the A_{mush} values of 10^6 and 10^8 and about 0.93 for $A_{mush} = 10^4$ (Fig. 3a), while at the end of established discharging time (2100 s) the melting fraction reaches the same value of about 0.41 for the three A_{mush} values considered (Fig. 3b). In charge phase, the difference between the three cases exists, even if it is not so evident. During melting, as previously stated, the heat transfer is strongly influenced by convection. In fact, an increase of A_{mush} involves a decrease of the convective rate with a consequent melting fraction drop/reduction. In discharge phase, almost the same behaviour was achieved since during solidification the heat transfer is dominated by conduction. This is also evident in Fig. 4 that shows the phase change evolution of the PCM during charge (a) and during discharge (b). Also in this case, the phase change front evolution during the charge phase is referred to Experiment 1 while the curves obtained during discharge are valid for both experiments. The figure shows a cross section of the TES system in which the inner tube is on the left side while the wall is on the right side. The lines represents the interface between liquid and solid PCM (reported at the centreline of the mushy zone, i.e. $MF = 0.5$) that moves from the centre (the inner tube) to the outer wall during the charge phase, and the interface between solid and liquid PCM during discharge phase. At the beginning of both charge and discharge processes, the transition front starts to form at the top of the TES system, where the HTF enters, along the entire length of the inner tube and around the fins. It is found that natural convection in the melted region, as well as the A_{mush} value, considerably influence the interface shape and motion during the melting process while during solidification the same behaviour of the phases evolution profile was detected for all cases considered. Fig. 4(a) shows the phase evolution of the PCM during charge for Experiment 1 considering different value of the mushy zone constant. At the beginning, the process is dominated by conduction. The liquid-solid interface moves almost parallel to the heating surface (the inner tube), then when the liquid phase increases, the influence of the natural convection becomes stronger. After 500 seconds, the convection heat transfer has a higher contribution in melting and helps increasing the heat transfer rate within the PCM domain. It is also possible to notice that the different values of the mushy zone constant have an influence on the shape of the

phase change front. In general, the presence of gravity, non-uniform temperature field and heterogeneous density generate a buoyancy force in the liquid PCM domain which determines the particular shape of the solid-liquid interface. In this case, the different shapes of the melting front were induced by the different values of viscosity obtained by Eq. (10) which is a function of A_{mush}. In fact, for values of A_{mush} of 10^6 and 10^8 the phase evolution presents the same behaviour while for $A_{mush} = 10^4$, differences on shape and motion were observed. A value of $A_{mush} = 10^4$ determines a downward curvature of the phase change front during melting process clearly noticeable after 1000 s (Fig. 4a) even if, as said before, this was not related to large differences in melting fraction rate. An increase in A_{mush} leads to an increase of the PCM viscosity and, consequently, of the diffusive term in Eq. (6) which dominates over the convective term.

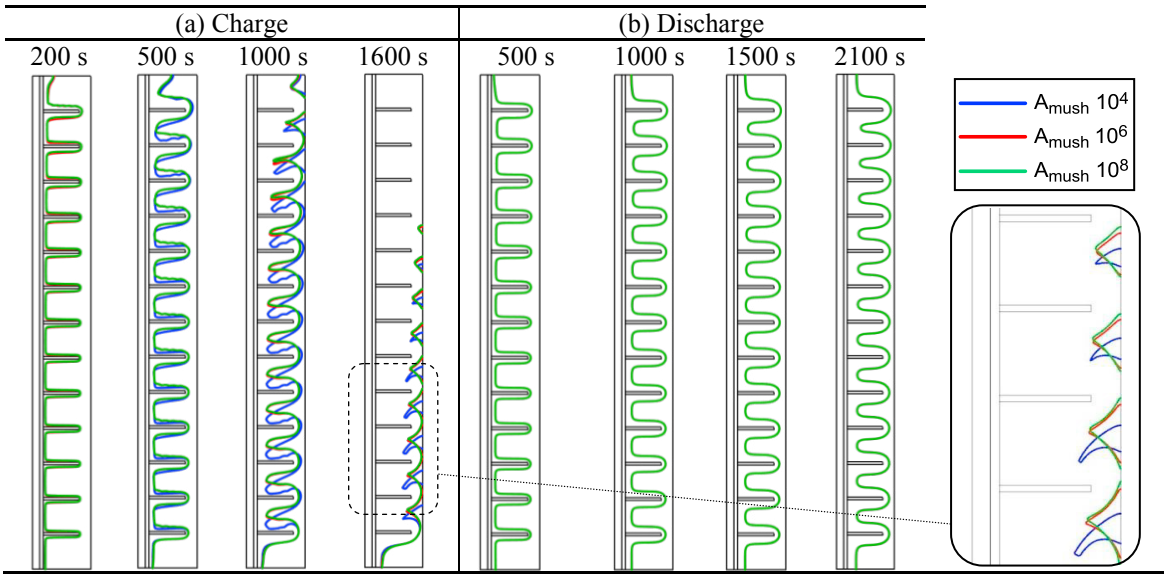

Fig. 4. Phase evolution during charge for Experiment 1 (a) and during discharge for both the experiments (b).

This means that, for low A_{mush} values, the shape of the melting front depends on both the heat transfer mechanisms (conduction and convection), while for high values of A_{mush}, conduction plays an important role in the formation and motion of this front. For the discharge phase (Fig. 4b), the three cases considered present very similar results. After 2100 seconds the solid-liquid interface is approximately in the same position also considering the different values of the mushy zone constant selected. In fact, in this case, conduction dominates the heat transfer process, thus the influence of natural convection is very low.

4. Conclusions

A numerical model was developed in the COMSOL Multiphysics environment to simulate a latent heat thermal energy storage system based on the configuration of a finned double tube heat exchanger, filled with paraffin RT35 as PCM. The analysis of the influence of the mushy zone constant (A_{mush}) on the melting and solidification behaviour of the PCM was presented by adopting three different values of the parameter A_{mush}, equal to 10^4, 10^6 and 10^8. In order to evaluate the influence of the heat transfer by convection during charge and discharge processes, a comparison with the results obtained with two experimental tests, performed in the laboratories of the University of Lleida, Spain, was carried out. Overall, a good agreement with the experimental temperature profiles during charge and discharge phase was obtained for the three different values of the mushy zone constant considered. During charge phase, the numerical temperature profiles present the same trend and a small difference was detected at the end of the process. It was found that smaller the A_{mush} value, higher the temperature due to the decrease of the mushy-zone area and the consequent increase of the natural convection effects. Conversely, no relevant difference on temperature profile, was observed by varying the constant A_{mush} during the discharge phase since, in the solidification process, conduction dominates the heat transfer process. The influence of the mushy zone constant was analyzed also in terms of melting fraction and phase change front evolution during both charge and discharge

processes. Concerning the melting fraction, a small difference between, about 2% the three cases was observed in the charge process, since during melting the heat transfer is strongly influenced by convection. Differently, almost the same behaviour of the three cases was obtained in the discharge process, since during solidification the heat transfer is dominated by conduction. Furthermore, it was found that the value of A_{mush} influences the interface shape and motion during the phase transition process. In fact, for values of A_{mush} of 10^6 and 10^8 the phase evolution presents the same behaviour while for $A_{mush} = 10^4$, a downward curvature of the phase change front was attained during the melting process. During the solidification process, the three cases considered present very similar results. At the end of the established discharging time, the solid-liquid interface is approximately in the same position also considering the different values of A_{mush} selected. In fact, in this case, conduction dominates the heat transfer process, thus the influence of natural convection is very low. Finally, it is important to emphasize that this paper provides only a preliminary discussion of the effects of the mushy zone constant on numerical simulation problems related to phase change heat transfer phenomena including natural convection. Further work is necessary to identify the proper value of A_{mush} not only considering other important factors such as the variation of the temperature range transition and other PCM characteristics, but also performing more in-depth experimental tests.

Acknowledgements

The work was partially funded by the Spanish government (ENE2015-64117-C5-1-R (MINECO/FEDER)). Jaume Gasia and Prof. Luisa F. Cabeza would like to thank the Catalan Government for the quality accreditation given to their research group (2014 SGR 123). GREA is certified agent TECNIO in the category of technology developers from the Government of Catalonia. This project has received funding from the European Commission Seventh Framework Programme (FP/2007-2013) under Grant agreement Nº PIRSES-GA-2013-610692 (INNOSTORAGE) and from the European Union's Horizon 2020 research and innovation programme under grant agreement No 657466 (INPATH-TES). Jaume Gasia would like to thank the Departament d'Universitats, Recerca i Societat de la Informació de la Generalitat de Catalunya for his research fellowship (2017 FI_B1 00092).

References

[1] Farid, Mohammed M., Amar M. Khudhair, Siddique Ali K. Razack, Said Al-Hallaj (2004) "A review on phase change energy storage: materials and applications." *Energy Conversion and Management* 45 (2004): 1597-1675.
[2] Longeon, Martin, Adèle Soupart, Jean-François Fourmigué, Arnaud Bruch, Philippe Marty (2013) "Experimental and numerical study of annular PCM storage in the presence of natural convection" *Applied Energy* 112 (2013): 175-184.
[3] Ismail, Kamal A.R., Maria das Graças E. da Silva (2003) "Numerical solution of the phase change problem around a horizontal cylinder in the presence of natural convection in the melt region." *International Journal of Heat and Mass Transfer* 46 (2003): 1791-1799.
[4] Faghri, Amir, Yuwen Zhang (1996) "Heat transfer enhancement in latent heat thermal energy storage system by using the internally finned tube" *International Journal of Heat and Mass Transfer* 39 (1996): 3165-3173.
[5] Waghmare, Avinash V, Ashok T. Pise (2015) "Numerical investigation of concentric cylinder latent heat storage with / without gravity and buoyancy" *Energy Procedia* 75 (2015): 3133–3141.
[6] Ismail Kamal A. R., L.M. Sousa, F. A. M. Lino (2015) "Solidification of PCM around Curved Tubes Including Natural Convection Effects." *International Journal of Energy Engineering* 5 (2015): 57-74.
[7] Shokouhmand, Hossein, Babak Kamkari (2013) "Experimental investigation on melting heat transfer characteristics of lauric acid in a rectangular thermal storage unit." *Experimental Thermal and Fluid Science* 50 (2013): 201–222.
[8] Shmueli, H, G. Ziskind, R. Letan (2008) "Investigation of Melting in a Vertical Circular Tube: Local Heat Fluxes." *SME. Heat Transfer Summer Conference, Heat Transfer* 2 (2008): 511–515.
[9] Groulx, Dominic, Ali C. Kheirabadi (2015) "The Effect of the Mushy-Zone Constant on Simulated Phase Change Heat Transfer". *ICHM International Symposium on Advances in Computational Heat Transfer* (2015).
[10] Kumar, Arun, S. K. Krishna (2017) "Influence of Mushy Zone Constant on Thermohydraulics of a PCM." *Energy Procedia* 109 (2017): 314–321.
[11] Medrano, Marc, M. O. Yilmaz, M. Nogués, I. Martorell, J. Roca, L. F. Cabeza (2009) "Experimental evaluation of commercial heat exchangers for use as PCM thermal storage systems." *Applied Energy* 86 (2009): 2047–2055.
[12] Rahimi, M., A. A. Ranjbar, D. D. Ganji, K. Sedighi, M. J. Hosseini (2014) "Experimental Investigation of Phase Change inside a Finned-Tube Heat Exchanger" *Journal of Engineering* (2014): 1-11.
[13] Rahimi, M., A. A. Ranjbar, D. D. Ganji, K. Sedighi, M. J. Hosseini, R. Bahrampoury (2014) "Analysis of geometrical and operational parameters of PCM in a fin and tube heat exchanger." *International Communications in Heat and Mass Transfer* 53 (2014): 109–115.
[14] Groulx, Dominic, R. Murray (2011) "Modeling Convection During Melting of a Phase Change Material". *Proceeding of the COMSOL Conference Boston* (2011).
[15] Groulx, Dominic, Wilson Ogoh (2009) "Solid-Liquid Phase Change Simulation Applied to a Cylindrical Latent Heat Energy Storage System." *Proceeding of the COMSOL Conference Boston*. (2009).
[16] Groulx, Dominic, F. Samara, P. H. Biwole (2012) "Natural Convection Driven Melting of Phase Change Material: Comparison of Two Methods." *Proceeding of the COMSOL Conference Boston* (2012): 1-8.